Supporting Information

Multiferroicity Engineered by Co^{2+} Substitution in Hybrid Ferroelectrics

Ya-Ru Kong,[a] Xiao-Lin Zhao,[a] Dong-Sheng Shao,*[a] Wei Ye,[a] Weihua Ning,*[b] Zheng-Fang Tian,[c] Hong-Bin Luo,[a] Xiao-Ming Ren*[a]

[a] State Key Laboratory of Materials-Oriented Chemical Engineering and College of Chemistry and Molecular Engineering, Nanjing Tech University, Nanjing 211816, P. R. China. E-mail: shaods@njtech.edu.cn, xmren@njtech.edu.cn

[b] State Key Laboratory of Bioinspired Interfacial Materials Science, Institute of Functional Nano & Soft Materials (FUNSOM), Soochow University, Suzhou, 215123 P. R. China. E-mail: whning@suda.edu.cn

[c] Hubei Key Laboratory for Processing and Application of Catalytic Materials, Huanggang Normal University, Huanggang 438000, P. R. China

Contents

Figures

Tables

References

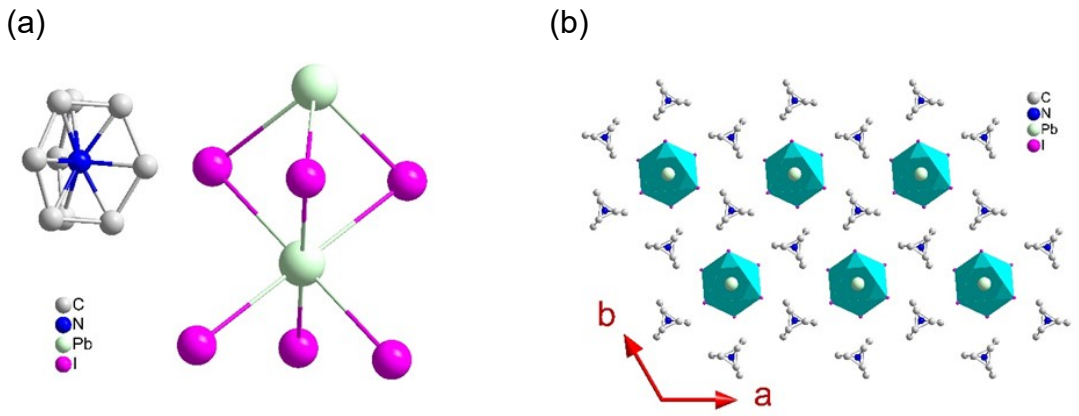

Figure S1. The crystal structure of $TMAPbI_3$ (a) asymmetric unit and (b) packing structure along with c-axis.

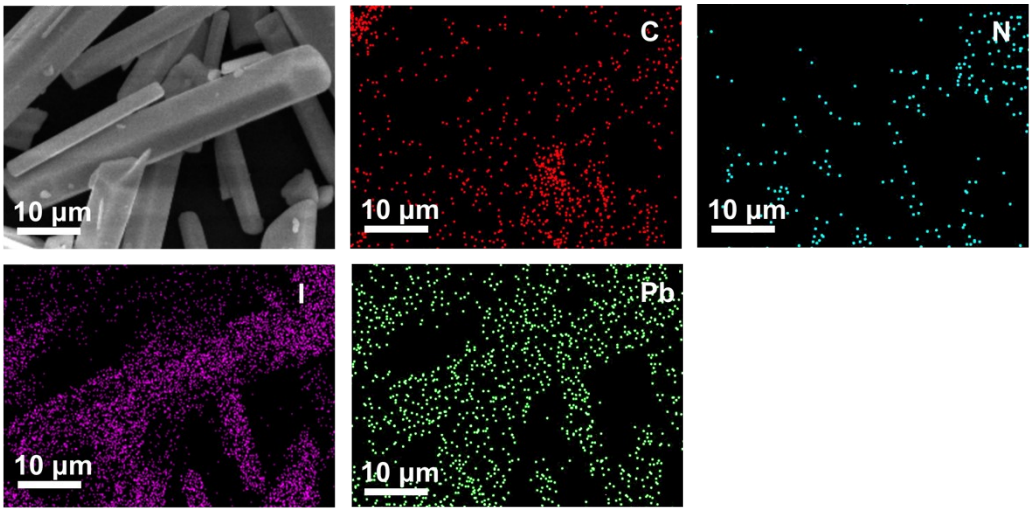

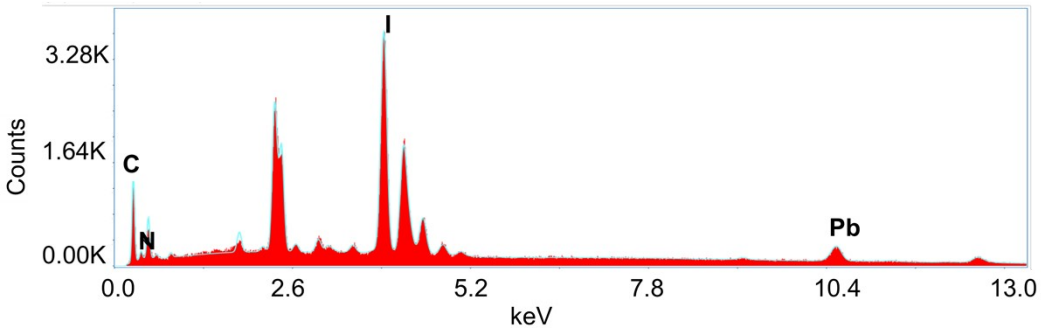

Element	Weight percentage	MDL	Atomic percentage	Net strength	Error %	R	A	F
C K	21.05	0.48	72.91	23.60	11.46	0.7183	0.1311	1.0000
N K	2.12	0.45	6.28	2.95	19.08	0.7255	0.0677	1.0000
I L	42.28	0.54	13.86	173.71	4.65	0.8129	0.7624	1.0080
Pb L	34.56	3.25	6.94	21.25	14.19	0.9404	0.9723	1.0458

Figure S2. FESEM images, EDS mapping and EDS spectra of $TMAPbI_3$.

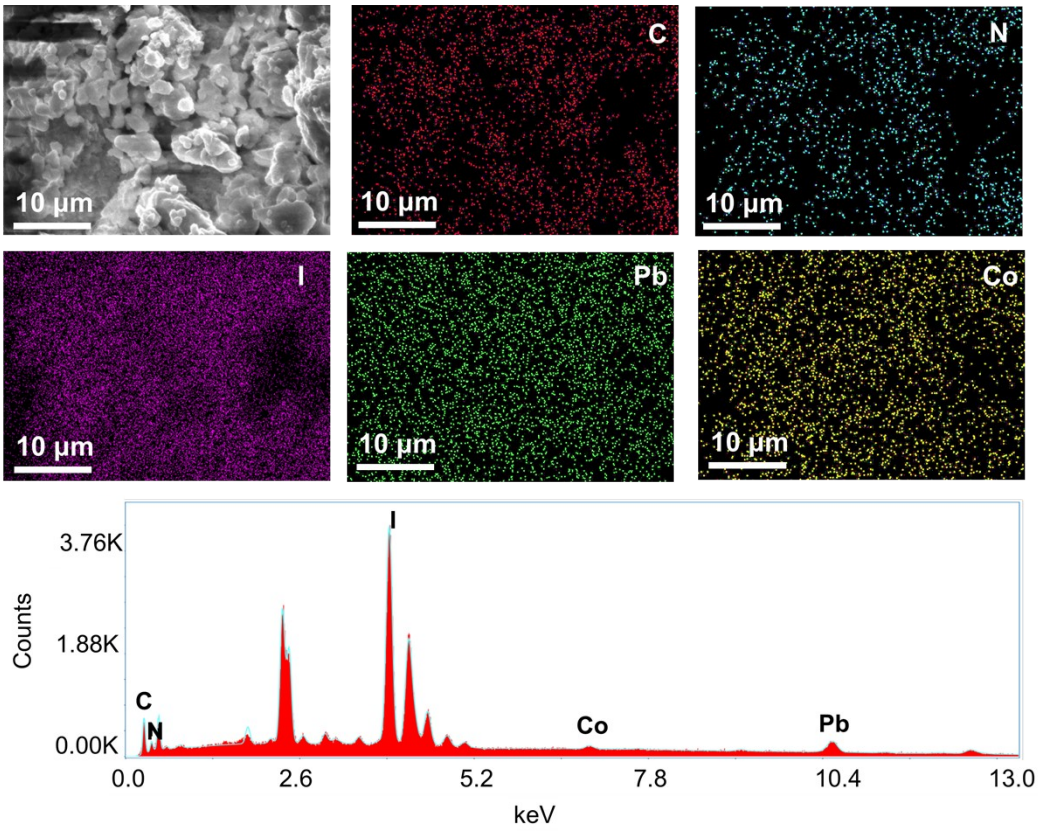

Element	Weight percentage	MDL	Atomic percentage	Net strength	Error %	R	A	F
C K	10.01	0.78	52.10	12.13	13.27	0.6886	0.1226	1.0000
N K	2.36	0.37	10.53	4.98	18.07	0.6949	0.0888	1.0000
Co K	0.75	0.43	0.80	4.86	30.83	0.8218	0.8574	1.0951
I L	54.21	0.60	26.71	253.33	4.61	0.7821	0.7522	1.0078
Pb L	32.67	3.58	9.86	23.48	18.19	0.9283	0.9665	1.0457

Figure S3. FESEM images, EDS mapping and EDS spectra of $TMA_{1-x}Pb_{1-x}Co_xI_{3-x}$ (x = 0.03).

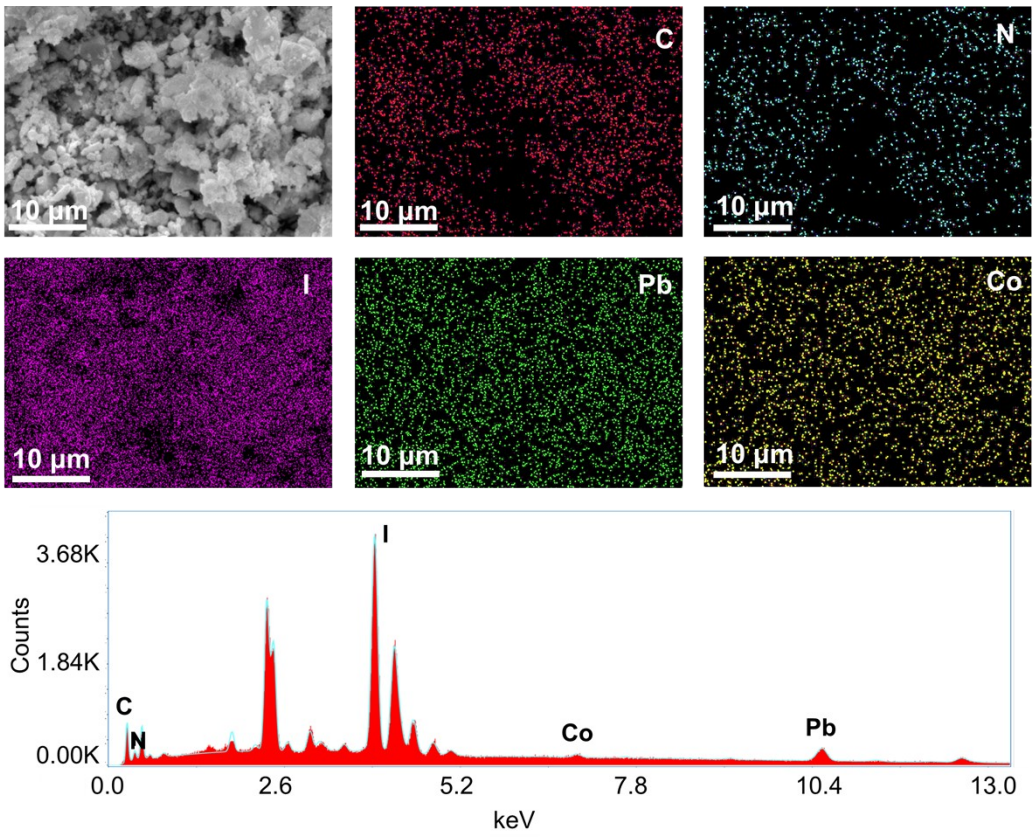

Element	Weight percentage	MDL	Atomic percentage	Net strength	Error %	R	A	F
C K	9.90	0.88	52.52	12.31	13.38	0.6863	0.1211	1.0000
N K	2.14	0.37	9.71	4.60	18.37	0.6924	0.0873	1.0000
Co K	0.76	0.42	0.82	5.10	30.74	0.8195	0.8578	1.0975
I L	52.12	0.66	26.17	250.47	4.72	0.7795	0.7454	1.0079
Pb L	35.09	3.44	10.79	26.21	17.11	0.9273	0.9664	1.0455

Figure S4. FESEM images, EDS mapping and EDS spectra of $TMA_{1-x}Pb_{1-x}Co_xI_{3-x}$ (x = 0.07).

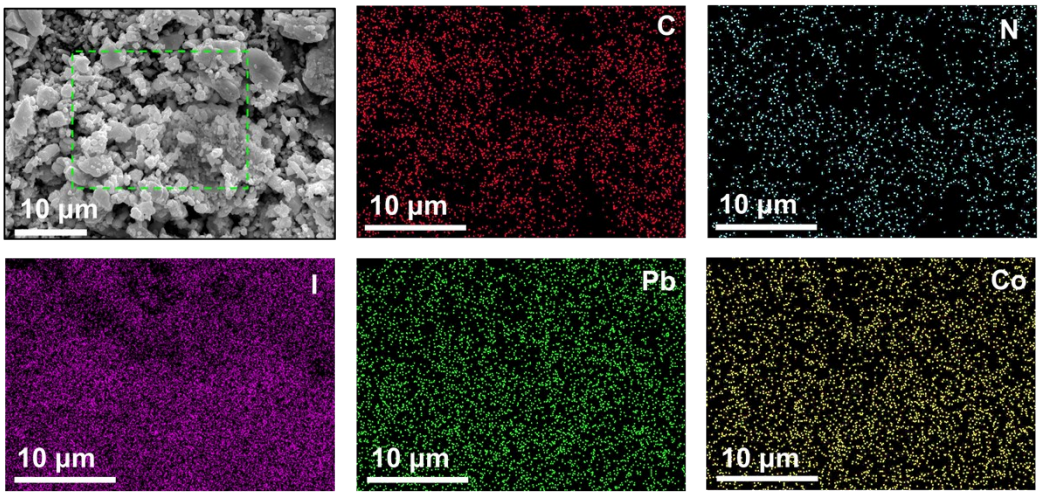

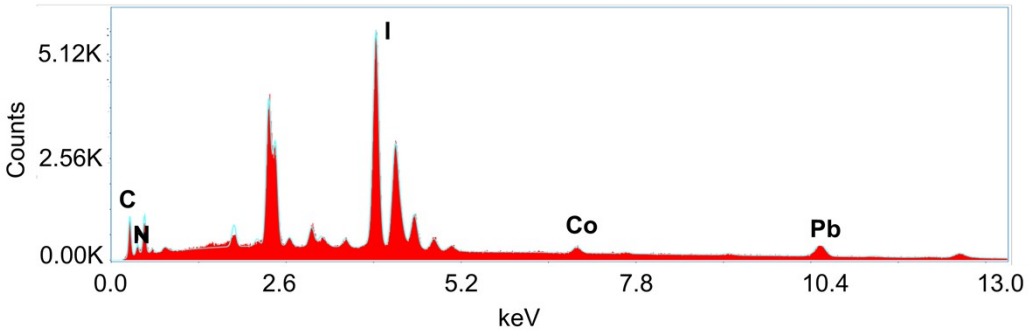

Element	Weight percentage	MDL	Atomic percentage	Net strength	Error %	R	A	F
C K	10.55	0.73	53.28	14.67	12.79	0.6907	0.1219	1.0000
N K	2.44	0.33	10.56	5.83	15.83	0.6970	0.0870	1.0000
Co K	1.39	0.34	1.43	10.41	20.31	0.8238	0.8601	1.0959
I L	52.12	0.56	24.92	280.82	4.46	0.7843	0.7515	1.0079
Pb L	33.50	2.78	9.81	27.75	14.75	0.9292	0.9669	1.0454

Figure S5. FESEM images, EDS mapping and EDS spectra of $TMA_{1-x}Pb_{1-x}Co_xI_{3-x}$ (x = 0.10).

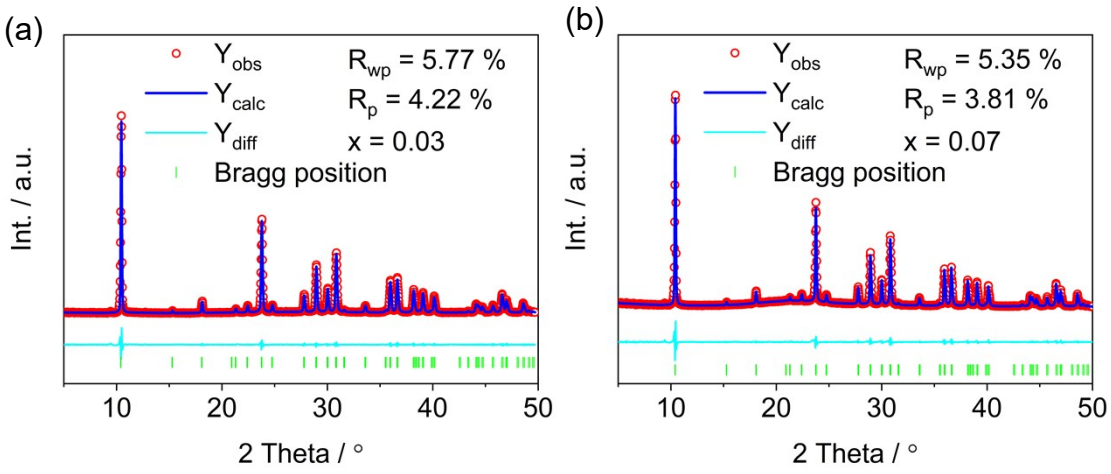

Figure S6. Pawley refinement of $TMA_{1-x}Pb_{1-x}Co_xI_{3-x}$ (a) x = 0.03 and (b) x = 0.07.

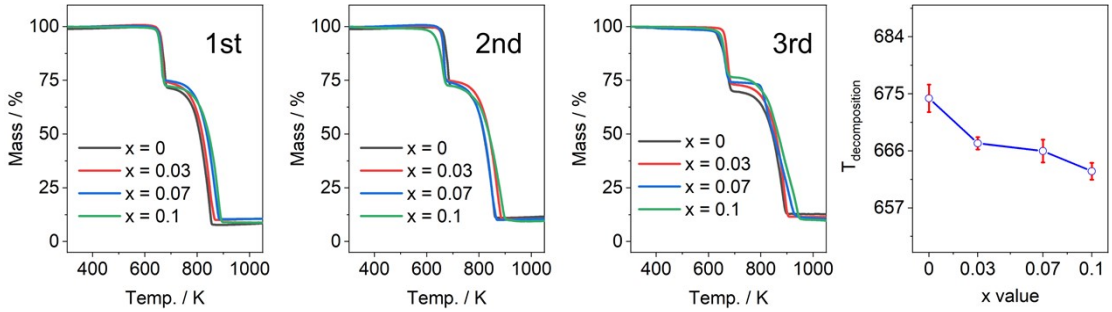

Figure S7. TG and error bar of decomposition temperature for all samples from three repeated measurements.

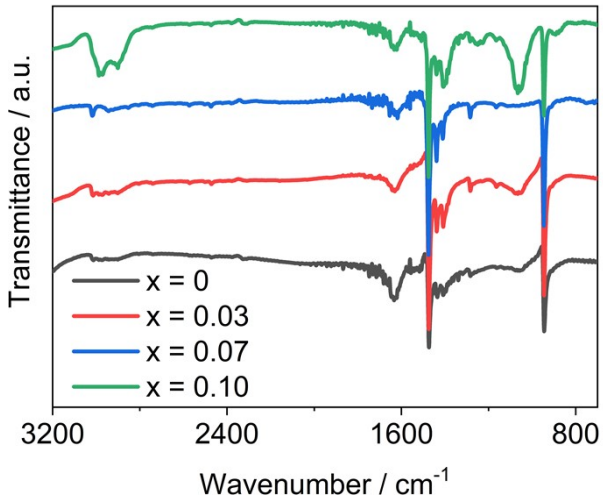

Figure S8. FT-IR spectra of $TMA_{1-x}Pb_{1-x}Co_xI_{3-x}$ (x = 0–0.10).

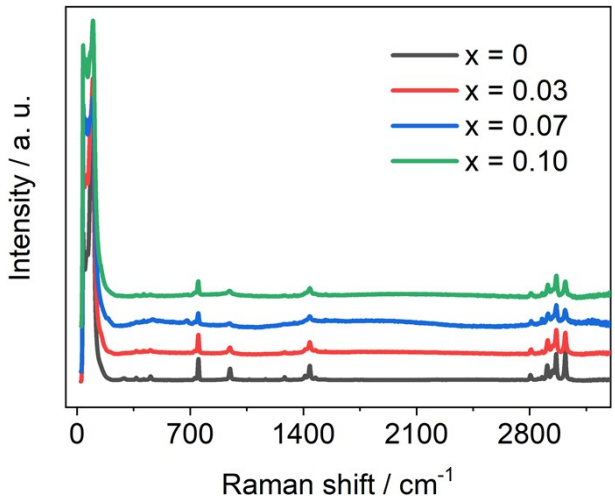

Figure S9. Raman spectra of $TMA_{1-x}Pb_{1-x}Co_xI_{3-x}$ (x = 0–0.10).

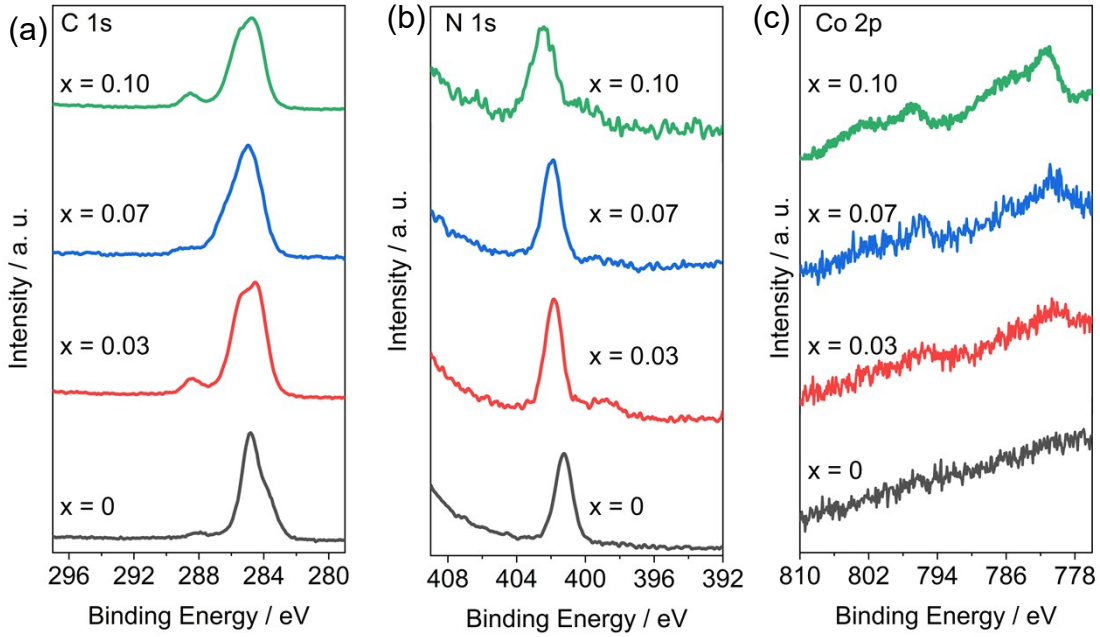

Figure S10. XPS spectra of $TMA_{1-x}Pb_{1-x}Co_xI_{3-x}$ (x = 0 – 0.10), (a) C 1s, (b) N1s and (c) Co 2p.

(c)

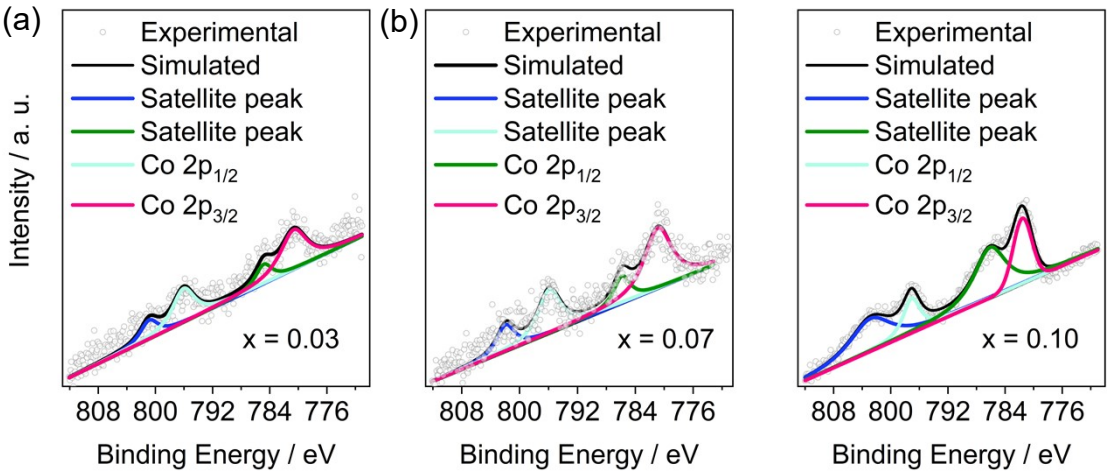

Figure S11. Simulated XPS spectrum of Co $2p_{1/2}$ and Co $2p_{3/2}$ from $TMA_{1-x}Pb_{1-x}Co_xI_{3-x}$, (a) x = 0.03, (b) x = 0.07, (c) x = 0.10.

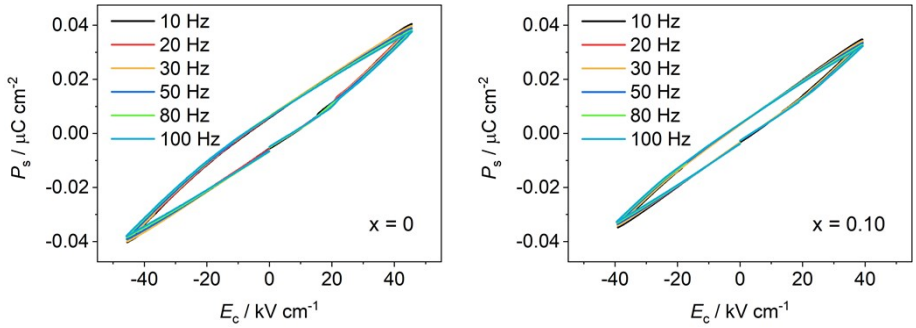

Figure S12. P–E loops for $TMA_{1-x}Pb_{1-x}Co_xI_{3-x}$ (x = 0 and 0.10) hybrids at 160 K and at different frequencies.

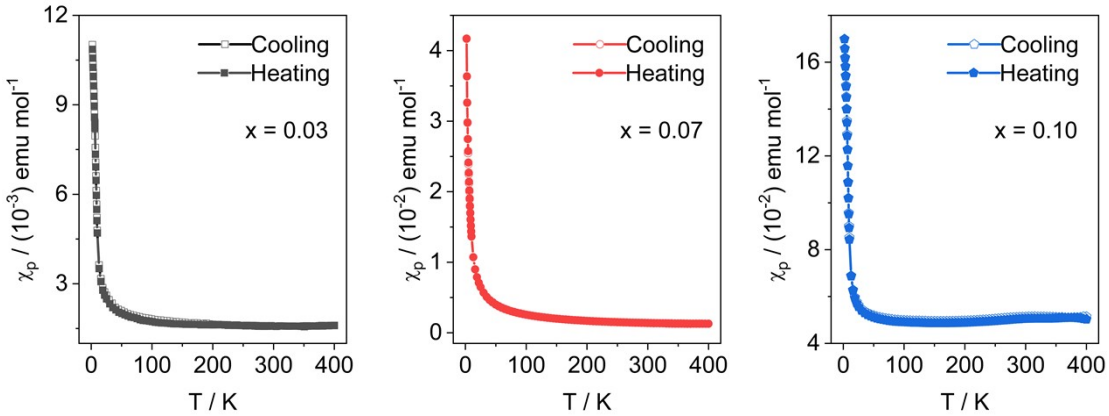

Figure S13. Plots of molar paramagnetic susceptibility χ_p *versus* temperature for $TMA_{1-x}Pb_{1-x}Co_xI_{3-x}$ with x = 0.03–0.10 range in 2–400 K.

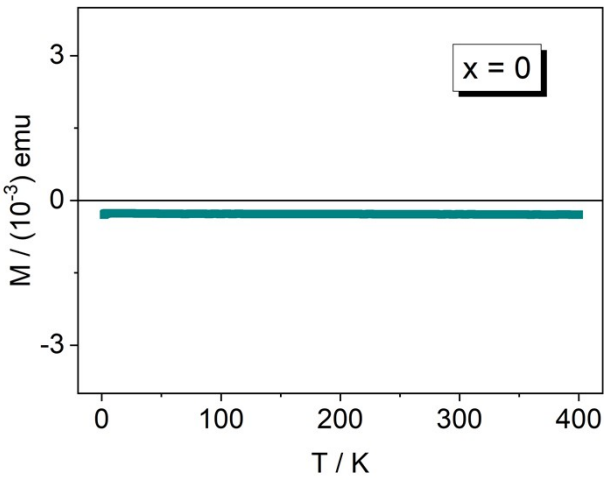

Figure S14. The molar magnetic susceptibility of $TMAPbI_3$

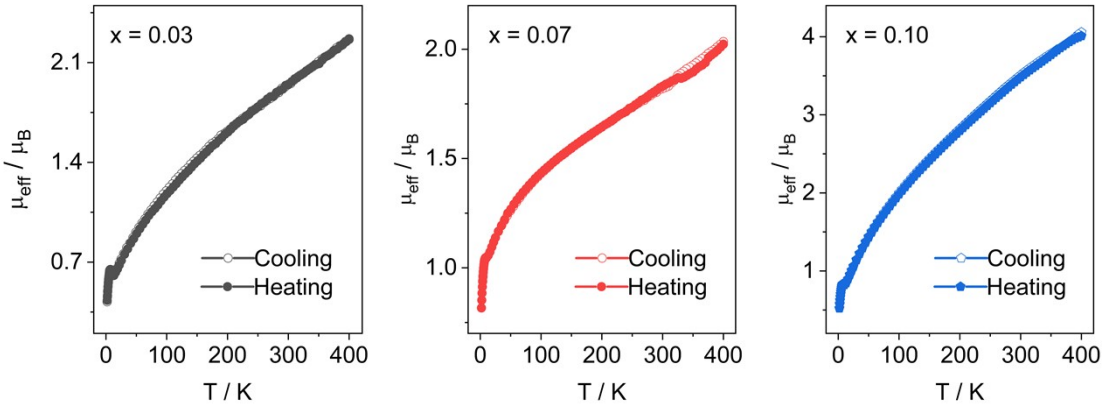

Figure S15. Plots of molar paramagnetic susceptibility μ_{eff} *versus* temperature for $TMA_{1-x}Pb_{1-x}Co_xI_{3-x}$ with x = 0.03–0.10 range in 2–400 K.

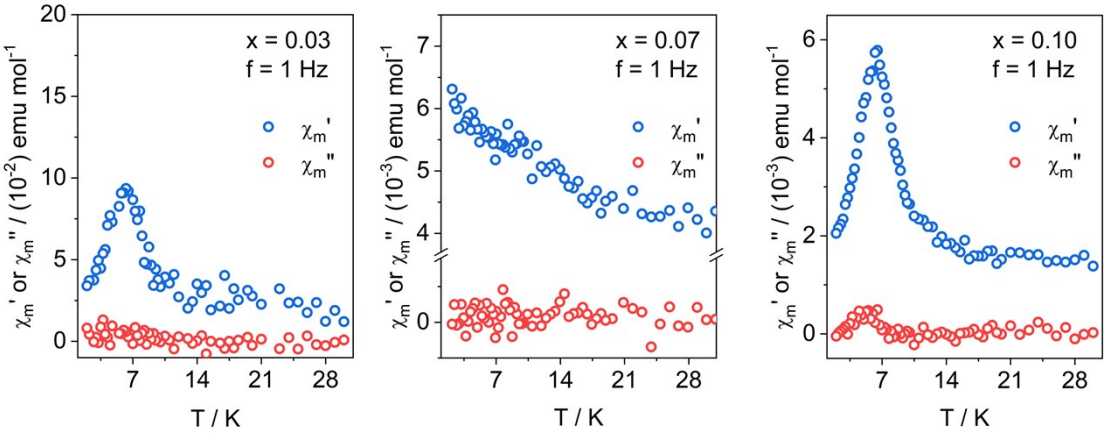

Figure S16. Temperature dependences of AC magnetic susceptibility χ_m' and χ_m'' in the frequency of 1 Hz for $TMA_{1-x}Pb_{1-x}Co_xI_{3-x}$ with x = (a) 0.03, (b) 0.07 and (c) 0.10.

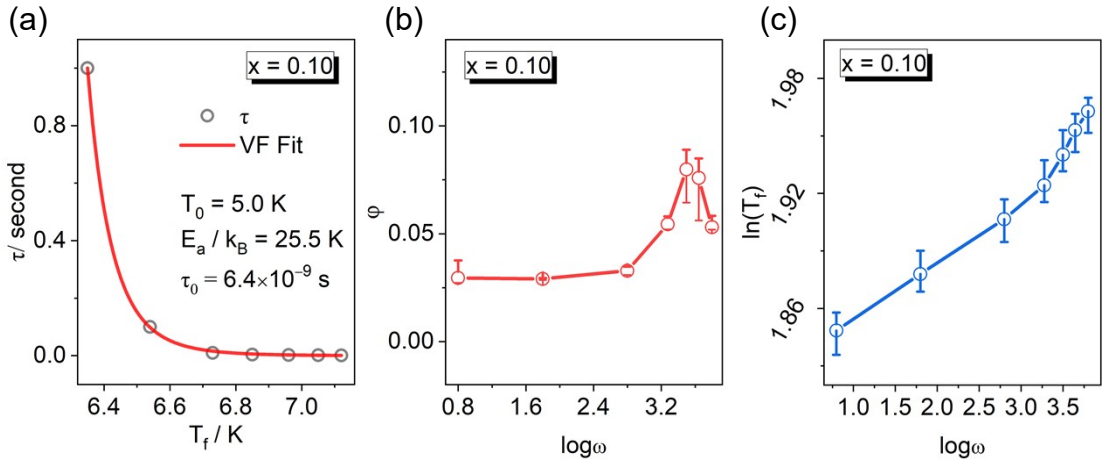

Figure S17. (a) Vogel–Fulcher (VF), (b) plot of φ vs. logω and (c) Plot of $\ln(T_f)$ vs. logω fit for $TMA_{1-x}Pb_{1-x}Co_xI_{3-x}$ (x = 0.10).

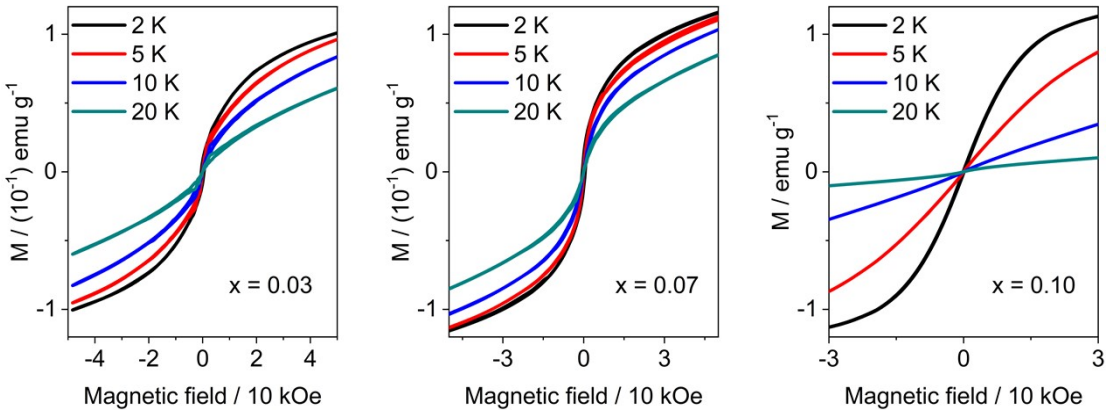

Figure S18. Magnetization *vs*. applied DC field curves for $TMA_{1-x}Pb_{1-x}Co_xI_{3-x}$ with x = 0.03–0.10 at 2–20 K.

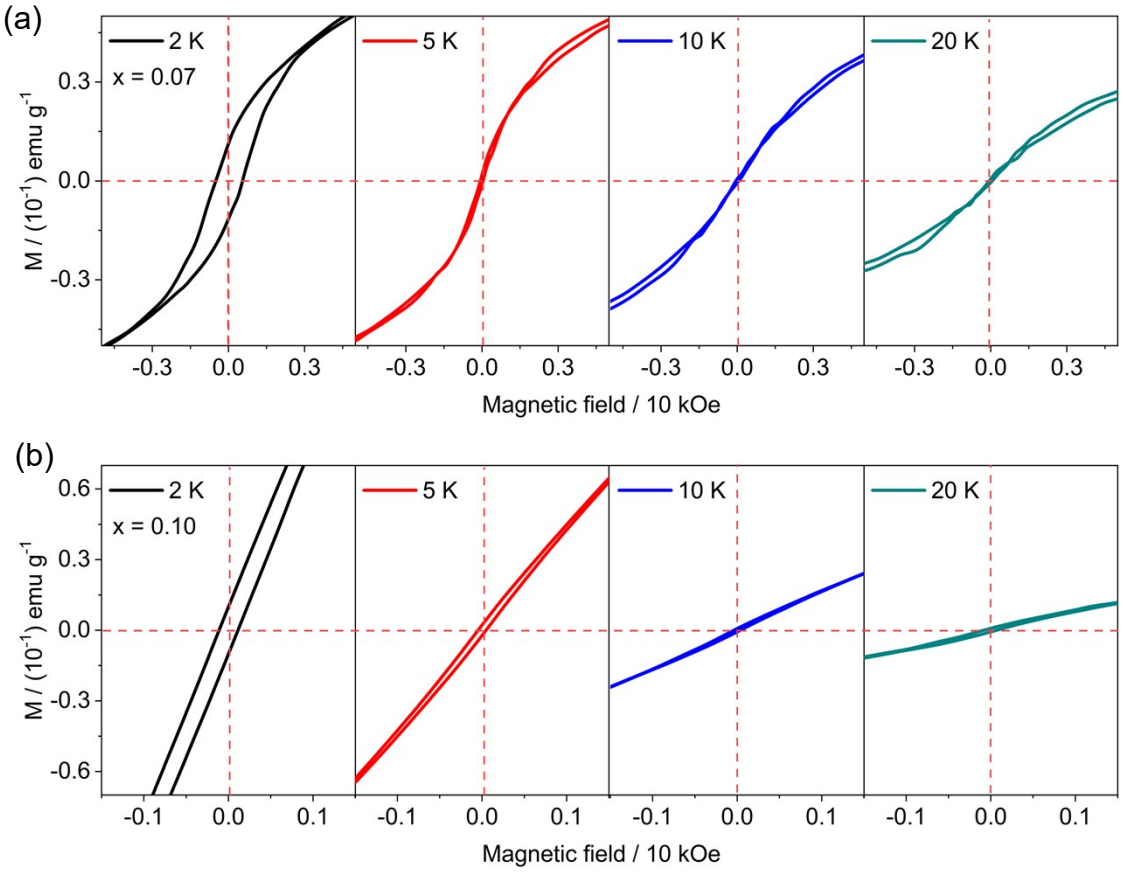

Figure S19. Magnetization *vs*. applied DC field curves for $TMA_{1-x}Pb_{1-x}Co_xI_{3-x}$ with (a) x = 0.07 and (b) x = 0.10 at 2–20 K.

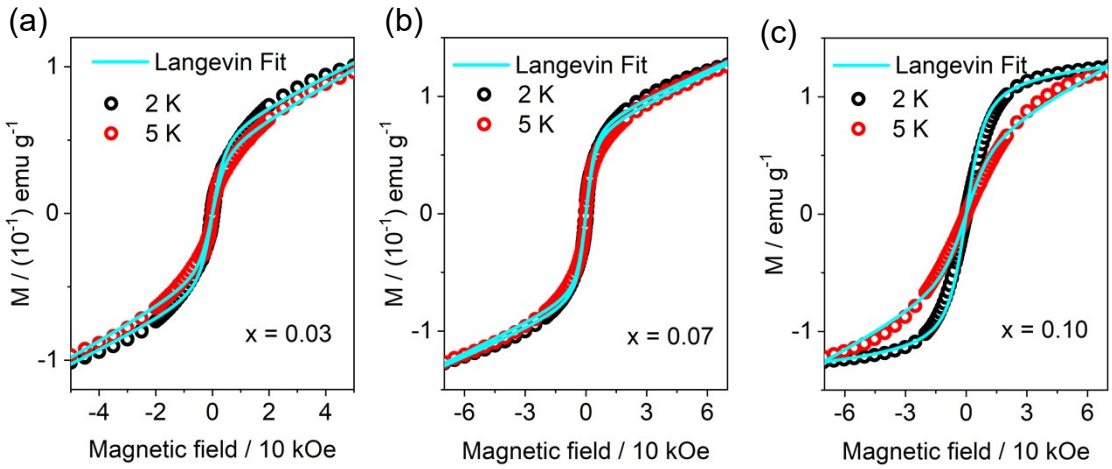

Figure S20. Fits of magnetization vs. magnetic field for $TMA_{1-x}Pb_{1-x}Co_xI_{3-x}$, (a) x = 0.03, (b) x = 0.07, (c) x = 0.10 at 2 K and 5 K.

Table S1. Molar ratio of Co to Pb in $TMA_{1-x}Pb_{1-x}Co_xI_{3-x}$ (x = 0–0.10) in form of x:(1-x)

$TMA_{1-x}Pb_{1-x}Co_xI_{1-x}$(x = 0-0.10)					
Sample		0	0.03	0.07	0.10
Feed ratio	Pb	/	0.99	0.95	0.90
	Co	/	0.01	0.05	0.10
ICP results	Pb	/	0.97	0.93	0.90
	Co	/	0.03	0.07	0.10

Table S2. Detailed vibrational assignments in IR spectrum for $TMA_{1-x}Pb_{1-x}Co_xI_{3-x}$ (x = 0–0.10)[1-3]

Observed frequencies (cm^{-1})	Approx. mode descriptions
3024 (s)	C–H asymmetric stretching
2975 (bm)	C–H symmetric stretching
1475 (vs)	C–H asymmetric deformation vibration
1435 (vs)	C–H symmetric deformation vibration
1407 (m)	C–H symmetric deformation vibration
1283 (w)	C-N stretching
945 (vs)	CH_3 rocking

Intensities: s – strong; bm – broad weak; vs – very strong; m –medium; w – weak; sh – shoulder.

Table S3. Detailed vibrational assignments in Raman spectrum for $TMA_{1-x}Pb_{1-x}Co_xI_{3-x}$ (x = 0–0.10)[4,5]

	Observed wavenumber (cm^{-1})	Approx. mode descriptions
Inorganic moiety	98 (w)	A_{1g} stretching vibration of Pb–I
	87 (sh)	Lattice vibration
	60 (m)	I–Pb–I bending vibration
	39 (s)	

Intensities: vs – very strong; m –medium; s – strong; w – weak; sh – shoulder.

Table S4. The X-ray photoelectron binding energy values of N 1s, Pb $4f_{5/2}$ and Pb $4f_{7/2}$, Co $2p_{1/2}$ and Co $2p_{3/2}$, I $3d_{3/2}$ and I $3d_{5/2}$ from $TMA_{1-x}Pb_{1-x}Co_xI_{3-x}$ (x = 0–0.10)

Element		E_b / eV				Ref.
		x = 0	x = 0.03	x = 0.07	x = 0.1	
N 1s	/	401.27	401.82	402.47	401.95	6
Pb 4f	$4f_{5/2}$	142.03	142.63	143.43	142.71	6
	$4f_{7/2}$	137.13	137.73	138.53	137.81	
Co 2p	$2p_{1/2}$	/	795.26	797.10	795.81	7
	$2p_{3/2}$	/	780.26	782.10	780.81	
I 3d	$3d_{3/2}$	629.36	629.92	630.74	630.06	8
	$3d_{5/2}$	617.86	618.42	619.24	618.56	

Table S5. Parameters obtained by fit of M–H plots at different temperatures for $TMA_{1-x}Pb_{1-x}Co_xI_{3-x}$ (x = 0.03–0.10)

x	0.03		0.07		0.1	
Temperature / K	2	5	2	5	2	5
M_s / emu g^{-1}	0.057	0.046	0.079	0.073	1.218	0.671
$\mu \times 10^{-6}$ / μ_B	1.701	4.027	1.807	4.505	0.843	1.462
$\chi \times 10^{-6}$ / emu g^{-1}	0.945	1.083	0.751	0.808	1.485	9.020

References

1. C. W. Young, J. S. Koehler and D. S. McKinney, *J. Am. Chem. Soc.*, 1947, **69**, 1410–1415. 1
2. K. M. Harmon, I. Gennick and S. L. Madeira, *J. Phys. Chem.*, 1974, **78**, 2585–2591. 1
3. M. Pal, A. Agarwal, M. B. Patel and H. D. Bist, *J. Raman Spectrosc.*, 1984, **15**, 211–216. 1
4. M. A. Hossain, F. Ahmed and J. P. Srivastava, *Phys. status solidi A*, 1995, **151**, 299–304. 1
5. J. G. Contreras, G. V. Seguel, B. Ungerer, W. F. Maier and F. J. Hollander, *J. Mol. Struct.*, 1983, **102**, 295–304. 1
6. J. Chastain and R. C. King Jr, *Perkin-Elmer Corporation*, 1992, **40**, 25. 1
7. W. Xu, L. Zheng, X. Zhang, Y. Cao, T. Meng, D. Wu, L. Liu, W. Hu and X. Gong, *Adv. Energy Mater.*, 2018, **8**, 1703178. 1
8. Z. Zheng, A. Liu, S. Wang, Y. Wang, Z. Li, W. M. Lau and L. Zhang, *J. Mater. Chem.*, 2005, **15**, 4555–4559.